

## Ca<sup>2+</sup>-Activated K<sup>+</sup> Channels of Human and Rabbit Erythrocytes Display Distinctive Patterns of Inhibition by Venom Peptide Toxins

C. Brugnara<sup>1</sup>, C.C. Armsby<sup>1</sup>, L. De Franceschi<sup>2</sup>, M. Crest<sup>3</sup>, M.-F. Martin Euclaire<sup>3</sup>, S.L. Alper<sup>4</sup>

<sup>1</sup>Departments of Pathology and Laboratory Medicine, The Children's Hospital, 300 Longwood Avenue, Boston, MA 02115

<sup>2</sup>Department of Internal Medicine, University of Verona, Verona, Italy

<sup>3</sup>Laboratoires de Neurobiologie and d'Ingenierie des Proteines, Centre National de la Recherche Scientifique, Marseille, France

<sup>4</sup>Molecular Medicine and Renal Units, Beth Israel Hospital and Department of Cell Biology and Medicine, Harvard Medical School, 330 Brookline Avenue, Boston, MA 02215

Received: 13 January 1995/Revised: 31 March 1995

**Abstract.** Despite recent progress in the molecular characterization of high-conductance Ca<sup>2+</sup>-activated K<sup>+</sup> (maxi-K) channels, the molecular identities of intermediate conductance Ca<sup>2+</sup>-activated K<sup>+</sup> channels, including that of mature erythrocytes, remains unknown. We have used various peptide toxins to characterize the intermediate conductance Ca<sup>2+</sup>-activated K<sup>+</sup> channels (Gardos pathway) of human and rabbit red cells. With studies on K<sup>+</sup> transport and on binding of <sup>125</sup>I-charybdotoxin (ChTX) and <sup>125</sup>I-kaliotoxin (KTX) binding in red cells, we provide evidence for the distinct nature of the red cell Gardos channel among described Ca<sup>2+</sup>-activated K<sup>+</sup> channels based on (i) the characteristic inhibition and binding patterns produced by ChTX analogues, iberiotoxin (IbTX) and IbTX-like ChTX mutants, and KTX (1–37 and 1–38 variants); (ii) the presence of some properties heretofore attributed only to voltage-gated channels, including inhibition of K transport by margatoxin (MgTX) and by stichodactyla toxin (StK); (iii) and the ability of scyllatoxin (ScyTX) and apamin to displace bound <sup>125</sup>I-charybdotoxin, a novel property for K<sup>+</sup> channels. These unusual pharmacological characteristics suggest a unique structure for the red cell Gardos channel.

**Key words:** Charybdotoxin — Iberiotoxin — Kaliotoxin — Margatoxin — Stichodactyla toxin — Scyllatoxin — Apamin — Gardos channel — Potassium channel — Red cell

## Introduction

The Ca<sup>2+</sup>-activated K<sup>+</sup> channel of the red cell, also known as the Gardos channel (Gardos, 1959), plays an important role in the dehydration of sickle erythrocytes (Bookchin, Ortiz & Lew, 1991; Lew et al., 1991; Brugnara, De Franceschi & Alper, 1993b) and in protecting red cells from swelling and lysis when complement is activated (Halperin, Brugnara & Nicholson-Weller, 1989a). Therefore, the relationship between the structure of different K<sup>+</sup> channel inhibitors and their effects on channel function has relevance not only for basic red cell physiology but also for its possible therapeutic applications in sickle cell disease and other erythroid dyscrasias.

The red cell Gardos channel is an intermediate-conductance K<sub>Ca</sub> channel (Hamill, 1983; Gryorczyk, Schwartz & Passow, 1984; Latorre et al., 1989; Christopherson, 1991). The molecular structure of this class of channels remains unknown, and patch-clamp analysis of the red cell membrane remains technically challenging. Therefore, pharmacological characterization of the Gardos channel continues to represent a major mode of comparison with other K<sub>Ca</sub> channels. Various small molecule inhibitors of the red cell Gardos channel have been described: Quinine (ID<sub>50</sub> = 5 μM in K<sup>+</sup>-free medium, 100 μM in 5 mM K<sup>+</sup> medium; Reichstein & Rothstein, 1981), carbocyanine (ID<sub>50</sub> = 20–50 nM, Simons, 1976), nifedipine (ID<sub>50</sub> = 4 μM; Kaji, 1990), nitrendipine (ID<sub>50</sub> = 130 nM; Ellory et al., 1992) and clotrimazole (CLT; ID<sub>50</sub> = 50 nM in normal erythrocytes; Alvarez, Montero & Garcia-Sancho, 1992; ID<sub>50</sub> 51 ± 15 nM in sickle erythrocytes, Brugnara et al. 1993b). However, the most potent blocker characterized to date is the scorpion venom

peptide toxin, charybdotoxin (Wolff et al., 1988; Brugnara, De Franceschi & Alper, 1993a).

Charybdotoxin (ChTX), a protein isolated from the venom of the scorpion *Leiurus quinquestriatus* (Gimenez-Gallego et al., 1988), is a 4.3 kDa polypeptide which inhibits numerous  $\text{Ca}^{2+}$ -activated and voltage-gated  $\text{K}^+$  channels (Miller et al., 1985; Gimenez-Gallego et al., 1988; Deutsch et al., 1991). The three-dimensional structure of the peptide has been solved by NMR (Bontems et al., 1991) and the recombinant gene product has been overexpressed in *E. Coli* (Park, Haudorff & Miller, 1991). A radioiodinated derivative of ChTX has been used to study toxin binding in different cell types which express toxin-sensitive channel activity (Vasquez et al., 1989; Deutsch et al., 1991; Brugnara et al., 1993a). However, since ChTX interacts not only with  $\text{Ca}^{2+}$ -activated  $\text{K}^+$  channels, but also with some voltage gated  $\text{K}^+$  channels, binding data should be interpreted with caution especially in cells possessing multiple types of  $\text{K}^+$  channels. In contrast, ChTX can be considered a specific inhibitor of the  $\text{Ca}^{2+}$ -activated  $\text{K}^+$  channel (Gardos channel) in human and rabbit red cells, since these cells do not express classic voltage-gated  $\text{K}^+$  channels (Brugnara et al., 1993a). For this reason, the erythrocyte offers a valuable, supplemental experimental model in which to characterize the pharmacology of  $\text{K}^+$  channel inhibitory peptide toxins, and in which measured effects can be attributed with confidence to interactions with  $\text{Ca}^{2+}$ -activated  $\text{K}^+$  channels.

Kaliotoxin (KTX) was originally described as an inhibitor of  $\text{Ca}^{2+}$ -activated  $\text{K}^+$  channels in nerve cells from the mollusc *Helix pomatia* (65 pS) and in rabbit coeliac ganglia sympathetic neurons (150 pS) with a  $K_d$  of 10–20 nM (Crest et al., 1992). Since binding of  $^{125}\text{I}$ -KTX to rat brain synaptosomes was displaced by dendrotoxin, Romi et al. (1993) suggested that KTX also blocks some voltage-gated  $\text{K}^+$  channels. This hypothesis was recently confirmed within mammalian cell lines expressing various recombinant voltage-dependent  $\text{K}^+$  channels (Grissmer et al., 1994). KTX-induced channel block is voltage-independent, suggesting mechanistic differences between channel blockade by KTX and by ChTX (Crest et al., 1992).

KTX was purified from the venom of the scorpion *Androctonus mauretanicus mauretanicus* as a single 4-KDa polypeptide chain initially thought to comprise 37 aa (Crest et al., 1992). A recent report suggests that native KTX is 38 aa in length, since an additional Lys could be identified at the toxin's C-terminus (Romi et al., 1993). KTX displays 44% amino acid sequence identity with charybdotoxin (ChTX), 44% identity with iberitoxin (IbTX), and 52% identity with noxiustoxin (NTX). KTX differs further from ChTX and IbTX in that its amino-terminus is unblocked (Crest et al., 1992). However, KTX differs from the recently described *Leiurus quinquestriatus* toxin, agitoxin 1 (AgTX1), in only

two of 38 residues (Garcia et al., 1994), showing that KTX and the several agitoxins comprise a toxin subfamily.

IbTX is a selective inhibitor in bovine aortic smooth muscle preparations of both the  $\text{Ca}^{2+}$ -activated  $\text{K}^+$  channel (maxi-K) and of specific  $^{125}\text{I}$ -ChTX binding (Galvez et al., 1990). IbTX binds to the outside of the channel, where its association constant is markedly decreased by external  $\text{K}^+$  (Candia, Garcia & Latorre, 1992). IbTX is less positively charged than ChTX, though sharing 68% sequence identity. The 3-dimensional NMR structure of IbTX has been solved (Johnson & Sugg, 1992). We have shown that whereas IbTX inhibited neither  $\text{Ca}^{2+}$ -activated  $\text{K}^+$  transport nor  $^{125}\text{I}$ -ChTX binding in human red cells, in rabbit red cells IbTX inhibited both  $\text{K}^+$  transport and  $^{125}\text{I}$ -ChTX binding, although with much lower potency than displayed by ChTX (Brugnara et al., 1993a).

Another toxin recently described as a selective inhibitor of voltage-gated  $\text{K}^+$  channels, margatoxin (MgTX; Garcia-Calvo et al., 1993; Bednarek et al., 1994;), has not been studied in human red cells. This toxin, which shares 79% amino acid identity with NTX and lesser degrees of identity with KTX (54%), ChTX (44%), and IbTX (41%), was inactive against the large conductance  $\text{Ca}^{2+}$ -gated  $\text{K}^+$  channels of aortic and tracheal smooth muscle and the intermediate conductance channel of human T-lymphocytes (Garcia-Calvo et al., 1993; Grissmer, Nguyen & Cahalan, 1993).

Additional toxins not previously characterized in red cells include: (i) Scyllatoxin (leiurotoxin I, ScyTX), which blocks small conductance (4–20 pS), apamin-sensitive,  $\text{Ca}^{2+}$ -activated  $\text{K}^+$  channels (Auguste et al., 1990; Pagel & Wemmer, 1994), and (ii) Stichodactyla toxin (StK), the first described peptide  $\text{K}^+$  channel blocker of marine origin (derived from sea anemones) which blocks voltage-gated, dendrotoxin (DTX)-sensitive,  $\text{K}^+$  channels (Karlsson et al., 1993; Kem et al., 1989).

Because ChTX and IbTX differ in their inhibitory properties on the  $\text{Ca}^{2+}$ -activated  $\text{K}^+$  channels of human and rabbit red cells (Brugnara et al., 1993a), it was of interest to compare systematically the effects of the above toxins and selected ChTX mutants on the  $\text{Ca}^{2+}$ -activated  $\text{K}^+$  channels of these two, otherwise similar cells. This comprehensive pharmacological characterization has detected additional significant differences between erythroid and other  $\text{Ca}^{2+}$ -gated  $\text{K}^+$  channels.

#### ABBREVIATIONS

AgTX	agitoxin
ChTX	charybdotoxin
DTX	dendrotoxin
EGTA	ethyleneglycol-bis-( $\beta$ -amino-ethylether) N,N'-Tetra-acetic Acid

IbTX	iberiotoxin
KTX	kaliotoxin
LIS	low ionic strength
MgTX	margatoxin
MOPS	3(N-morpholino) propanesulfonic Acid
NTX	noxiustotoxin
ScyTX	scyllatoxin
StK	stichodactyla toxin

## Materials and Methods

### DRUGS AND CHEMICALS

NaCl and KCl were purchased from Mallinckrodt, St. Louis, MO. Tris (hydroxymethyl) aminomethane (Tris), 3(N-morpholino) propanesulfonic Acid (MOPS), ethyleneglycol-bis-( $\beta$ -amino-ethylether) N,N'-Tetra-acetic Acid (EGTA), ouabain, octyl-phenoxy polyethoxyethanol (Triton X-100), apamin (95% pure by HPLC analysis, purified from bee venom), alfa-cellulose and microcrystalline cellulose were purchased from Sigma Chemical (St. Louis, MO). MgCl<sub>2</sub> and dimethyl-sulfoxide (DMSO) were purchased from Fisher Scientific (Fair Lawn, NJ). Choline chloride and A23187 were purchased from Calbiochem-Behring (La Jolla, CA). Sucrose was purchased from Serva Biochemicals, Paramus, NJ. Bovine Serum Albumin Fraction V was purchased from Boehringer Mannheim Biochemicals (Indianapolis, IN). Bumetanide was a gift from Leo Pharmaceutical Products (Ballerup, Denmark). All solutions were prepared using double-distilled water.

Synthetic charybdotoxin (ChTX), iberiotoxin (IbTX), scyllatoxin (ScTX) and stichodactyla toxin (StK) were purchased from Peptides International (Louisville, KY). Dendrotoxin (DTX) was purchased from BachemBioscience (King of Prussia, PA). <sup>125</sup>I-ChTX was purchased from New England Nuclear (Boston, MA). The 37 aa and 38 aa forms of KTX and <sup>125</sup>I-KTX were synthesized as previously described (Crest et al., 1992; Romi et al., 1993). Commercial KTX, 1-37 was obtained from Peptide International (lot 430226, KTX A) and from Bachem (B00622, KTX B). Margatoxin (MgTX) was kindly provided by Dr. Maria L. Garcia (Merck Research Laboratories, Rahway, NJ).

All peptide toxin preparations were dissolved in water and maintained as 20  $\mu$ M stock solutions at -70°C for no longer than 4 weeks.

### RED CELL PREPARATION

Blood was collected in heparinized Vacutainer tubes (Becton, Dickinson, Rutherford, NJ) from normal human donors or rabbits. Blood was depleted of leukocytes by passage through cotton and then centrifuged in a Sorvall refrigerated centrifuge (RC5B, Du Pont Instruments, Sorvall Biomedical, Newtown, CT) at 5°C for 10 min at 3,000  $\times$  g. The red cells were washed five times with a washing solution containing 152 mM choline chloride, 1 mM MgCl<sub>2</sub>, 10 mM Tris-MOPS, pH 7.40 at 4°C (Brugnara et al., 1993a).

### MEASUREMENT OF <sup>86</sup>Rb<sup>+</sup> INFLUX IN HUMAN RED CELLS

Red cells were incubated at room temperature for 90 min in a medium containing either 18 mM NaCl, 2 mM KCl, 230 mM sucrose (low ionic strength medium) or 140 mM NaCl, 2 mM KCl (physiologic salt concentration medium), at a concentration of 1  $\times$  10<sup>7</sup> cells/ml. Both media contained 10 mM tris-HCl, pH 8.0, 100 nM ouabain, 10  $\mu$ M bumetanide, 0.25% bovine serum albumin and the desired amount of toxin. At the end of the incubation, the cell suspension was spun at 3,000  $\times$  g for 10 min, the supernatant removed, and a smaller volume of medium con-

taining the Ca<sup>2+</sup> ionophore A23187 (60  $\mu$ mol/l cells), 50  $\mu$ M CaCl<sub>2</sub>, and <sup>86</sup>Rb<sup>+</sup> (5  $\mu$ Ci/ml) was added to a final Hct of 4-5%. Aliquots of this cell suspension were taken at specified times (0.5, 1, 2, 3, 4, 5, and 10 min for the time course experiments of Fig. 1 and 1, 3, and 5 min for all the other experiments) and spun in Eppendorf tubes containing 0.4 ml butyl-phthalate oil and 0.8 ml of medium with 5 mM EGTA. The supernatant and the upper layer of oil were carefully removed, and the cell pellet was counted in a gamma counter. Initial rates of <sup>86</sup>Rb<sup>+</sup> influx were obtained from the slope of the regression line of time versus red cell <sup>86</sup>Rb<sup>+</sup> uptake.

Flux inhibition curves by different toxins were fitted using the "Asymmetric sigmoid equation,"  $y = \min + (\max - \min)/(1 + (x/IC_{50})^{-P})$ , where  $x$  is the concentration of toxin,  $y$  is the flux expressed as percentage of control, max and min are expressed as 100 and 0%, respectively. The program Ultrafit v 2.1 (Elsevier) was used for curve fitting. IC<sub>50</sub> values were accepted when goodness of fit values were above 0.95. Inhibition curves for each toxin were calculated with 10 data points, each corresponding to the following concentration of toxin (nM): 0, 0.001, 0.01, 0.05, 0.1, 0.5, 1, 5, 10, and 50.

### MEASUREMENT OF <sup>125</sup>I-KTX AND <sup>125</sup>I-CHTX BINDING TO RED CELLS

White cells were removed by passing 0.8 ml of packed red cells through a 5 ml syringe containing a mixture of equal parts of alfa-cellulose and microcrystalline cellulose (Brugnara et al., 1993a). Red cells were washed three times in binding medium containing (in mM): 18 NaCl, 2 KCl, 10 tris-Cl, pH 8.0, 230 sucrose and 0.25% bovine serum albumin, and resuspended in this medium to a 15% Hct. The composition of this medium and the addition of bovine serum albumin have been shown to maximize specific binding and reduce nonspecific binding of <sup>125</sup>I-ChTX, respectively (Brugnara et al., 1993a). The cell suspension was added to 3.5 ml of binding medium containing <sup>125</sup>I-KTX or <sup>125</sup>I-ChTX to a final concentration of 1  $\times$  10<sup>7</sup> cells/mL, in the absence or presence of excess unlabeled KTX or ChTX. Tubes containing cell suspension were gently rotated for 90 min at 37°C. At the end of the incubation, aliquots of 1 ml were spun in an Eppendorf centrifuge and washed three times at 4°C with a solution containing 200 mM NaCl, 10 mM tris-Cl, pH 8.0. The pellets containing red cells were then lysed in 1 ml double distilled water containing 0.01% Acetoxon<sup>®</sup>, and counted in a gamma counter. Aliquots of binding medium were also counted prior to addition of cells and at the end of the binding assay.

Binding curves were fit to a hyperbolic isotherm, and inhibition and displacement curves were fit to an asymmetric sigmoid equation using the programs Ultrafit v. 2.1 (Elsevier) or Cricket-Graph III v. 1.1.

## Results

### EFFECTS OF SYNTHETIC PEPTIDE TOXINS ON CA<sup>2+</sup>-ACTIVATED <sup>86</sup>Rb FLUX INTO HUMAN RED CELLS

The effects of peptide toxins on the Ca<sup>2+</sup>-activated K<sup>+</sup> channel of human red cells were assessed by measuring <sup>86</sup>Rb<sup>+</sup> influx activated by A23187 (60  $\mu$ mol/L cells) in the presence of 0.05 mM CaCl<sub>2</sub>. The toxins studied included the 37 aa and 38 aa forms of KTX synthesized as previously described (Crest et al., 1992; Romi et al., 1993), two lots of commercial synthetic KTX 1-37 (A

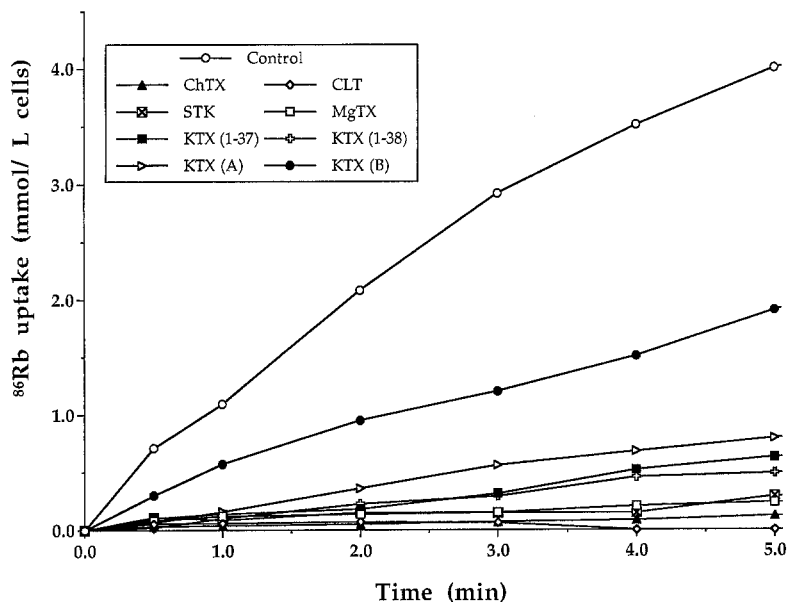


**Fig. 1.** Time course of inhibition of  $\text{Ca}^{2+}$ -activated  $^{86}\text{Rb}^+$  influx by venom peptide toxins (20 nM final concentration) and clotrimazole (10  $\mu\text{M}$ ). Red cells were incubated at room temperature for 30 min in a medium containing 18 mM NaCl, 2 mM KCl, 50  $\mu\text{M}$   $\text{CaCl}_2$ , 100 nM ouabain, 10  $\mu\text{M}$  bumetanide, and 10 mM tris-HCl, pH 8.0, at a concentration of  $1 \times 10^7$  cells/mL, in the presence of the  $\text{Ca}^{2+}$  ionophore A23187 (60  $\mu\text{mol/L}$  cells). At time zero, the specified inhibitor and  $^{86}\text{Rb}^+$  (5  $\mu\text{Ci/ml}$ ) were added.  $^{86}\text{Rb}^+$  influx was measured over 5-min incubation at room temperature.

and B, see Materials and Methods) and synthetic preparations of ChTX, IbTX, MgTX, ScyTX and StK.

The time course for inhibition of  $\text{Ca}^{2+}$ -activated  $^{86}\text{Rb}^+$  influx by these toxins (20 nM) and by clotrimazole (10  $\mu\text{M}$ , CLT; Alvarez et al., 1992; Brugnara et al., 1993b) is shown in Fig. 1. There was prompt inhibition by KTX, similar to that observed with ChTX and with CLT, two potent inhibitors of the  $\text{Ca}^{2+}$ -activated  $\text{K}^+$  channel of human red cells (Brugnara et al., 1993a; Alvarez et al., 1992). However, the degree of inhibition produced by similar concentrations of two commercial preparations of KTX (identified here as KTX A and KTX B) was markedly reduced compared to our own KTX (Crest et al., 1992; Romi et al., 1993). There was also substantial inhibition by MgTX and StK. ScyTX, in contrast, did not inhibit the Gardos channel (*not shown*, see Table 2).

The effects of ionic strength, pH and  $[\text{Ca}^{2+}]$  on the inhibitory effects of KTX, 1–37 and ChTX on  $\text{Ca}^{2+}$ -activated  $^{86}\text{Rb}^+$  influx were compared at single concentrations of the toxins. As shown in Table 1, external pH affected the magnitude of  $\text{Ca}^{2+}$ -activated  $^{86}\text{Rb}^+$  influx to a greater degree than its fractional inhibition by KTX or ChTX. At  $\text{pH}_o$  6.0 in low ionic strength conditions, channel activity was virtually absent, confirming the findings by Heinz & Hoffman (1990) but not those of Stampe & Vestergaard-Bogind (1985). The inhibitory effect of acid  $\text{pH}_o$  on  $\text{Ca}^{2+}$ -activated  $^{86}\text{Rb}^+$  influx was attenuated in saline, but fractional inhibition by either toxin remained independent of  $\text{pH}_o$ . Increasing external  $\text{Ca}^{2+}$  from 50  $\mu\text{M}$  to 1 mM had no significant effect either on  $\text{Ca}^{2+}$ -activated  $^{86}\text{Rb}^+$  influx or its inhibition by KTX or ChTX. Alkaline pH (8.0) was selected for most subsequent experiments.

The dose dependence of inhibition of the Gardos

pathway by the various toxins was studied in isotonic media of low (20 mM, sucrose substitution) and physiological (142 mM) salt concentrations. In the absence of A23187,  $^{86}\text{Rb}^+$  influx was unaffected by addition of toxins (*data not shown*). When the  $\text{Ca}^{2+}$ -dependent  $\text{K}^+$  channel was activated by A23187, marked inhibition of  $^{86}\text{Rb}^+$  influx into cells incubated in an isotonic 20 mM salt medium was observed with all toxins tested except IbTX, DTX, ScyTX, and apamin. The computed  $\text{ID}_{50}$  values for the various toxins are presented in Table 2. The  $\text{ID}_{50}$  values for KTX 1–37 ( $3.3 \pm 0.6$  nM;  $n = 3$ ) and for KTX 1–38 ( $5.0 \pm 2.0$  nM;  $n = 3$ ) were considerably less potent than for ChTX, ( $\text{ID}_{50}$  of  $14 \pm 2$   $\mu\text{M}$  in the same conditions,  $n = 3$ ). MgTX also showed high affinity inhibition of  $\text{Ca}^{2+}$ -activated  $\text{K}^+$  transport ( $\text{ID}_{50} = 0.79 \pm 0.11$  nM,  $n = 3$ ), with 98% inhibition by 20 nM MgTX. Two commercial preparations of KTX, 1–37 showed markedly reduced potency compared with our KTX preparation (Table 2, Fig. 1) synthesized as described (Crest et al., 1992; Romi et al., 1993).

As shown in Table 2, the inhibitory potency of KTX was decreased in normal saline. The KTX preparations tested (20 nM max concentration) showed marginal inhibition of  $\text{Ca}^{2+}$ -activated  $^{86}\text{Rb}^+$  influx in saline, whereas ChTX (82% inhibition at 20 nM,  $\text{ID}_{50}$  of  $5.4 \pm 1.9$  nM,  $n = 2$ ) and StK (59% inhibition at 20 nM,  $\text{ID}_{50}$  of  $24.5 \pm 4.5$  nM,  $n = 2$ ) showed significant but still incomplete inhibition. The two commercially available preparations of KTX 1–37 again showed reduced potency compared with our synthetic preparation. Neither MgTX nor IbTX inhibited  $\text{Ca}^{2+}$ -activated  $\text{K}^+$  transport at 20 nM concentrations in physiological saline medium. We also tested the effects of the mammalian brain  $\text{K}^+$  channel inhibitors dendrotoxin (DTX), scyllatoxin (ScyTX), and apamin on  $\text{Ca}^{2+}$ -activated  $^{86}\text{Rb}^+$  influx into red cells. Twenty nM

**Table 1.** The effect of pH, ionic strength, and external  $\text{Ca}^{2+}$  on the inhibition of  $\text{Ca}^{2+}$ -activated  $\text{K}^+$  transport by KTX, 1–37

	Total flux	$^{86}\text{Rb}^+$ Influx (mmol/liter cell $\times$ min)	
		KTX, 1-37 inhibition 2.5 nM (%)	ChTX inhibition 50 pM (%)
Low ionic strength medium			
pH 6.0	0.00 $\pm$ 0.0	0.00 $\pm$ 0.0 —	0.00 $\pm$ 0.0 —
pH 7.0	0.45 $\pm$ 0.07	0.29 $\pm$ 0.08 (36 $\pm$ 10%)	0.07 $\pm$ 0.05 (84 $\pm$ 60%)
pH 8.0	1.17 $\pm$ 0.08	0.72 $\pm$ 0.09 (38 $\pm$ 5%)	0.37 $\pm$ 0.23 (68 $\pm$ 42%)
Saline medium			
		2.5 nM	2.5 nM
pH 6.0	0.21 $\pm$ 0.29	0.15 $\pm$ 0.21 (29 $\pm$ 41%)	0.14 $\pm$ 0.19 (33 $\pm$ 45%)
pH 7.0	0.47 $\pm$ 0.29	0.37 $\pm$ 0.24 (21 $\pm$ 14%)	0.26 $\pm$ 0.17 (45 $\pm$ 29%)
pH 8.0	1.18 $\pm$ 0.01	0.87 $\pm$ 0.01 (26 $\pm$ 0.3%)	0.52 $\pm$ 0.12 (56 $\pm$ 13%)
Low ionic strength medium, pH 8.0			
		2.5 nM	50 pM
0.05 mM $\text{Ca}^{2+}$	1.17 $\pm$ 0.08	0.72 $\pm$ 0.09 (38 $\pm$ 5%)	0.37 $\pm$ 0.23 (68 $\pm$ 42%)
0.2 mM $\text{Ca}^{2+}$	1.21 $\pm$ 0.11	1.00 $\pm$ 0.11 (17 $\pm$ 2%)	0.61 $\pm$ 0.04 (50 $\pm$ 3%)
0.5 mM $\text{Ca}^{2+}$	1.26 $\pm$ 0.19	0.86 $\pm$ 0.03 (32 $\pm$ 1%)	0.58 $\pm$ 0.03 (54 $\pm$ 3%)
1 mM $\text{Ca}^{2+}$	1.23 $\pm$ 0.13	0.72 $\pm$ 0.12 (41 $\pm$ 7%)	0.53 $\pm$ 0.04 (57 $\pm$ 4%)

Data are means  $\pm$  SD of two separate experiments, each with triplicate determinations.

**Table 2.** Inhibition of  $\text{Ca}^{2+}$ -activated  $\text{K}^+$  transport into human red cells and displacement of specific  $^{125}\text{I}$ -ChTX binding by peptide toxins

	Inhibition of $^{86}\text{Rb}^+$ influx		Saline		$^{125}\text{I}$ -ChTX displacement	
	Low ionic strength % maximal inhibition	$\text{ID}_{50}(\text{app})$ (nM)	% maximal inhibition	$\text{ID}_{50}(\text{app})$ (nM)	Low ionic strength % maximal inhibition	$\text{ID}_{50}(\text{app})$ (nM)
ChTX	98 $\pm$ 1.8	0.014 $\pm$ 0.002	82 $\pm$ 4.5	5.4 $\pm$ 1.9	100 $\pm$ 4.8	0.3 $\pm$ 0.1
STK	99 $\pm$ 1.2	0.39 $\pm$ 0.19	59 $\pm$ 0.4	24.5 $\pm$ 4.5	89 $\pm$ 11	2.5 $\pm$ 1.6
MgTX	99 $\pm$ 0.7	0.79 $\pm$ 0.11	8 $\pm$ 14	n.d.	117 $\pm$ 14	2.6 $\pm$ 1.1
KTX,1–37	63 $\pm$ 3.5	3.3 $\pm$ 0.6	40 $\pm$ 0.6	n.d.	89 $\pm$ 7.8	1.1 $\pm$ 0.3
KTX,1–38	72 $\pm$ 4.2	5.0 $\pm$ 2.0	40 $\pm$ 0.4	n.d.	83 $\pm$ 9.2	4.2 $\pm$ 0.4
KTX,1–37A	32 $\pm$ 7.4	n.d.	16 $\pm$ 9.2	n.d.	66 $\pm$ 2.4	0.9 $\pm$ 0.6
KTX,1–37B	24 $\pm$ 6.0	n.d.	17 $\pm$ 7.8	n.d.	57 $\pm$ 5.1	2.4 $\pm$ 0.7
IbTX	0	n.d.	0	n.d.	0	n.d.
DTX	1.8 $\pm$ 0.1	n.d.	7.3 $\pm$ 11	n.d.	0 $\pm$ 0.2	n.d.
ScyTX	5.1 $\pm$ 6.7	n.d.	4.7 $\pm$ 6.7	n.d.	52 $\pm$ 12	23.6 $\pm$ 7.9
Apamin	3 $\pm$ 12	n.d.	0.7 $\pm$ 11	n.d.	42 $\pm$ 15	451 $\pm$ 856

“% maximal inhibition” represents fraction of maximal inhibition by ChTX produced by 50 nM toxin (20 nM for KTX,1–37 and 1–38, 100 nM for apamin) at low or physiological ionic strength, as indicated. Apparent  $\text{ID}_{50}$  values are toxin concentrations which inhibited 50% as well as did 50 nM ChTX.  $\text{ID}_{50}$  values were not calculated when maximum inhibitory effects were  $\leq 40\%$ ; n.d., not determined.

concentrations of these toxins produced no significant inhibition of transport whether in conditions of low or physiological ionic strength.

Extracellular salt inhibits the binding of ChTX to the Gardos channel (Brugnara et al., 1993a), presumably by electrostatic interactions of the toxin with the channel (Deutsch et al., 1991). Moreover, intracellular  $\text{K}^+$  is known to trans-inhibit ChTX binding to the skeletal muscle maxi- $\text{K}^+$  channel via interaction with toxin residue K27 (Park & Miller, 1992), presumably by an electrostatic “knock-off” mechanism. It was therefore of interest to examine the effects of extracellular and intra-

cellular  $\text{K}^+$  on the inhibitory potency of KTX and ChTX in the red cell.

To study the effect of external  $\text{K}^+$  on toxin inhibition of  $\text{K}^+$  transport, external  $\text{K}^+$  concentration was varied between 2 and 140 mM and the inhibition of transport by submaximal concentrations of ChTX and KTX was studied. Total ouabain- and bumetanide-resistant  $\text{Ca}^{2+}$ -activated  $^{86}\text{Rb}^+$  influx increased, as expected, with increasing external  $\text{K}^+$  (*not shown*). However, this increase in flux was associated with a progressive loss of inhibition by ChTX and by KTX, 1–38 (Fig. 2A). This experiment does not distinguish between direct effects of

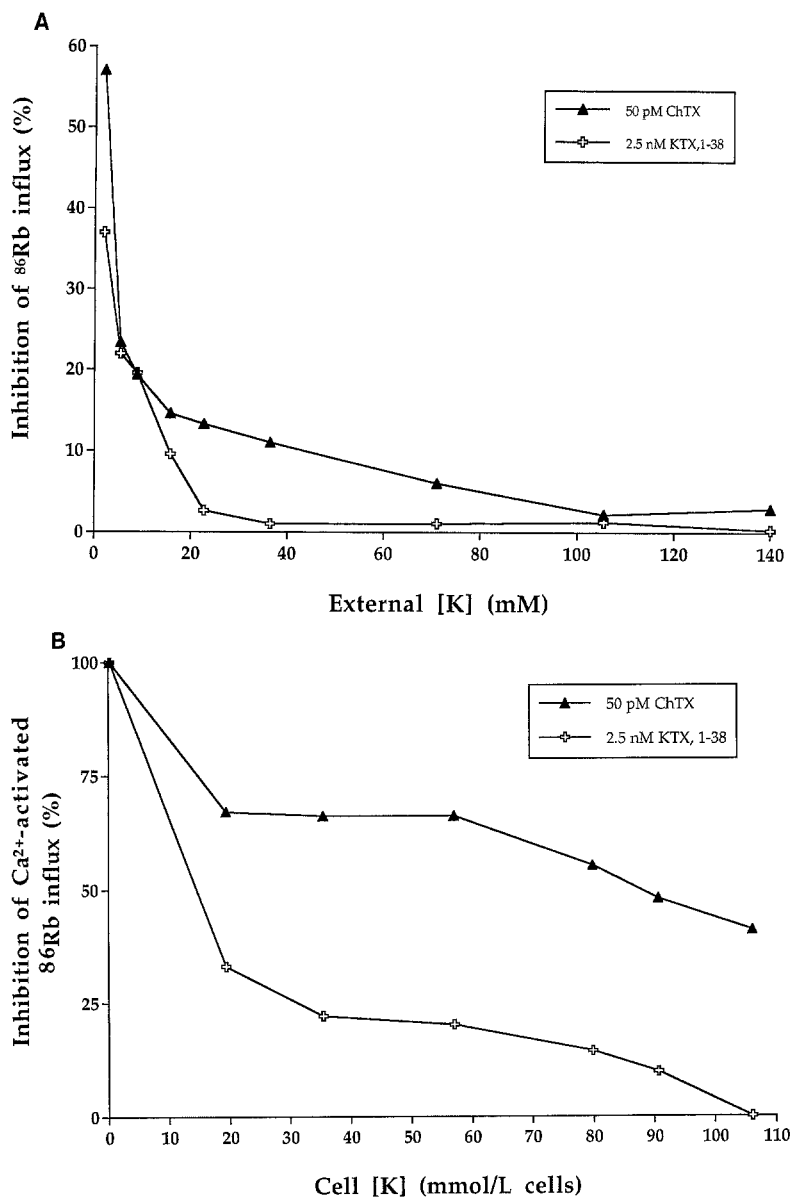


**Fig. 2.** Effect of external  $\text{K}^+$  (A) and internal  $\text{K}^+$  (B) on the inhibitory effect of 50 pM ChTX and 2.5 nM KTX, 1-38, on the  $\text{Ca}^{2+}$ -activated  $^{86}\text{Rb}^+$  influx into human red cells. Influxes were measured in media with physiologic ionic strength, pH 8.0. In A,  $^{86}\text{Rb}$  influx was measured into fresh cells at varying external  $\text{K}^+$  concentrations. Total  $^{86}\text{Rb}$  influx was 0.8 mmol/L cell  $\times$  min at 2 mM  $\text{K}^+$ , and increased to 3.8 mmol/L cell  $\times$  min at 140 mM  $\text{K}^+$ . In B,  $^{86}\text{Rb}$  influx was measured into cells containing varying amounts of  $\text{K}^+$ , at fixed external  $\text{K}^+$  (2 mM).  $^{86}\text{Rb}^+$  influx was 0.027 mmol/L cell  $\times$  min in cells containing 0.18 mmol  $\text{K}^+$ /L cells and increased to 1.38 mmol/L cell  $\times$  min in cells containing 106 mmol  $\text{K}^+$ /L cells. SD for all the data points was between 5 and 15% of the mean values of triplicate determinations.

external  $\text{K}^+$  and effects mediated by changes in  $E_m$ , since  $E_m$  also changes in response to increasing external  $\text{K}^+$  concentration, becoming progressively less inside-negative and reaching inside-positive values.

The effect of varying internal  $\text{K}^+$  was studied in cells treated with nystatin to obtain different intracellular  $\text{K}^+$  concentrations with  $\text{Na}^+$  replacement. Following removal of nystatin,  $\text{Ca}^{2+}$ -activated  $^{86}\text{Rb}^+$  influx was measured from media containing 2 mM  $\text{K}^+$ . As shown in Fig. 2B, increasing internal  $\text{K}^+$  induced a significant, biphasic reduction in the inhibitory effect of fixed high concentrations of ChTX and KTX. Fractional inhibition by the toxins of  $\text{Ca}^{2+}$ -activated  $^{86}\text{Rb}^+$  influx progressively decreased with rising internal  $\text{K}^+$  concentration in this experiment.  $E_m$  also changed throughout the experiment, being inside positive in the absence of internal  $\text{K}^+$

and becoming progressively more inside negative when internal  $\text{K}^+$  concentration was increased at the expense of  $\text{Na}^+$  (Halperin et al., 1989b). These data indicate that either or both an outwardly directed  $\text{K}^+$  gradient or elevations of external  $\text{K}^+$  similarly reduce the inhibitory potencies of ChTX and KTX.  $\text{K}^+$  dependence has also been shown in patch-clamp experiments (Grygorczyk & Schwarz, 1983). Since in our experimental conditions, high internal  $\text{K}^+$  was associated with inside-negative  $E_m$  and high external  $\text{K}^+$  with inside positive  $E_m$ , the observed reduction in inhibitory potency of ChTX and KTX by  $\text{K}^+$  was unlikely mediated by altered membrane potential alone.

The observed stimulation of  $\text{Ca}^{2+}$ -activated  $\text{K}^+$  flux by external  $\text{K}^+$  is compatible with a previous reports in intact human red cells (Heinz & Passow, 1980) and with

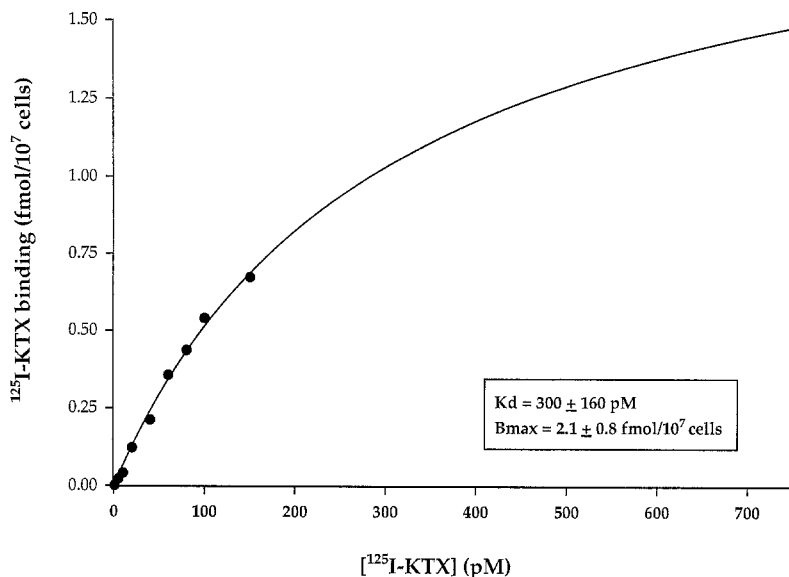


**Fig. 3.** Specific binding of  $^{125}\text{I}$ -KTX to human erythrocytes. Specific binding was calculated as the difference between  $^{125}\text{I}$ -KTX binding in the absence and presence of excess (20 nM) cold KTX. The curve was fit for a one-site ligand binding model. Curve fitting yielded a  $K_d$  of  $300 \pm 160$  pM and a capacity of  $2.1 \pm 0.8$  fmol/ $10^7$  cells, corresponding to  $126 \pm 48$  binding sites per red cell. SD for all the data points was between 5 and 15% of the mean value of triplicate determinations.

a reported increase in single channel conductance measured in excised red cell membrane patches (Christopherson, 1991).

#### SPECIFIC (DISPLACEABLE) BINDING OF $^{125}\text{I}$ -CHTX AND $^{125}\text{I}$ -KTX TO HUMAN RED CELLS

It was of interest to test the correspondence between inhibition of  $\text{Ca}^{2+}$ -activated  $^{86}\text{Rb}^+$  influx and displacement of  $^{125}\text{I}$ -KTX from human red cells. Our previous work with ChTX (Brugnara et al., 1993a) showed that the  $\text{ID}_{50}$  value for displacement of  $^{125}\text{I}$ -ChTX specific binding from human red cells (95 pM) was five times higher than the  $\text{ID}_{50}$  for inhibition of  $\text{Ca}^{2+}$ -activated  $^{86}\text{Rb}$  influx (21 pM) in low ionic strength conditions. The effects of increasing concentrations of KTX 1-37, KTX 1-38, MgTX, StK, and ChTX on the binding of  $^{125}\text{I}$ -ChTX to human red cells are summarized in Table 2. The concentration of  $^{125}\text{I}$ -ChTX used for these experiments was 50 pM. Curve-fitting analysis yielded  $\text{ID}_{50}$  values for displacement of bound  $^{125}\text{I}$ -ChTX of  $1.1 \pm 0.3$  nM (KTX, 1-37,  $n = 2$ ),  $4.2 \pm 0.4$  nM (KTX, 1-38,  $n = 2$ ),  $2.6 \pm 1.1$  nM (MgTX,  $n = 1$ ),  $2.5 \pm 1.6$  nM (StK,  $n = 2$ ) and  $0.3 \pm 0.1$  pM (ChTX,  $n = 3$ ). The value obtained for ChTX in these experiments is slightly higher than the one we had previously reported, using blood from a different individual (95 pM; Brugnara et al., 1993a). We confirmed the lack of effect of IbTX on ChTX binding to human red cells (Brugnara et al., 1993a), and in addition found no displacement of  $^{125}\text{I}$ -ChTX by 20 nM DTX.

Among the toxins studied here, iodinated derivatives have been described and characterized only for ChTX and KTX. Iodinated KTX has been used for studies in rat brain synaptosomes (Romi et al., 1993), but its effect in human red cells have not been reported. The binding

of  $^{125}\text{I}$ -KTX and its displacement by cold KTX or ChTX was studied in human red cells. Specific binding of 100 pM  $^{125}\text{I}$ -KTX (defined as that displaceable by 20 nM unlabeled KTX) was evaluated at different values of pH, ionic strength and external  $\text{Ca}^{2+}$  concentration, as reported in Table 1 for KTX-sensitive  $^{86}\text{Rb}$  influx. Table 3 shows that, as previously reported for  $^{125}\text{I}$ -ChTX (Brugnara et al., 1993a), there was a significant increase in specific binding in media with alkaline pH, in the absence of external  $\text{Ca}^{2+}$ , and with low ionic strength conditions. The binding of  $^{125}\text{I}$ -KTX (150 pM) could be specifically displaced by either KTX, 1-37 ( $\text{ID}_{50}$   $4.9 \pm 1.1$  nM) or ChTX ( $\text{ID}_{50}$   $8.2 \pm 4.0$  nM). Binding of  $^{125}\text{I}$ -KTX to red cells was examined at concentrations ranging from 1 pM to 150 pM in a  $\text{Ca}^{2+}$ -free, low ionic strength medium at pH 8.0. The binding curve was computer-fit to a single site model, yielding a  $K_{50}$  of  $300 \pm 160$  pM and a  $B_{\text{max}}$  of  $2.1 \pm 0.8$  fmol/ $10^7$  cells, corresponding to  $126 \pm 48$  binding sites per cell (Fig. 3). This  $B_{\text{max}}$  value is indistinguishable from values previously reported for  $^{125}\text{I}$ -ChTX binding to human red cells ( $120 \pm 36$  sites per cell; Brugnara et al., 1993a), supporting the hypothesis that the two iodotoxins recognize red cell binding sites which are identical or highly similar.

#### INHIBITORY EFFECTS OF CHTX MUTANTS ON THE $\text{Ca}^{2+}$ -ACTIVATED $\text{K}^+$ TRANSPORT OF HUMAN AND RABBIT ERYTHROCYTES

Though IbTX is more potent than ChTX in blockade of the maxi-K channel of vascular smooth muscle, it is less potent as a blocker of the Gardos channel. A series of recombinant ChTX preparations mutant in different single amino acid residues was used to search for one position in the toxin which might be responsible for the

**Table 3.** Specific binding of  $^{125}\text{I}$ -KTX (1–37) and the effect of pH, ionic strength, and external  $\text{Ca}^{2+}$ 

	$^{125}\text{I}$ -KTX binding (fmol/ $10^7$ cells)		
	Total	Nonspecific	Specific
Low ionic strength			
pH 6.0	0.515 $\pm$ 0.24	0.151 $\pm$ 0.11	0.364 $\pm$ 0.13
pH 7.0	0.939 $\pm$ 0.25	0.170 $\pm$ 0.06	0.769 $\pm$ 0.19
pH 8.0	1.535 $\pm$ 0.18	0.419 $\pm$ 0.16	1.116 $\pm$ 0.04
Normal saline			
pH 6.0	0.093 $\pm$ 0.04	0.041 $\pm$ 0.03	0.052 $\pm$ 0.04
pH 7.0	0.208 $\pm$ 0.01	0.070 $\pm$ 0.03	0.138 $\pm$ 0.03
pH 8.0	0.280 $\pm$ 0.12	0.120 $\pm$ 0.09	0.160 $\pm$ 0.08
Low ionic strength, pH 8.0			
0 $\text{Ca}^{2+}$	0.666 $\pm$ 0.23	0.219 $\pm$ 0.02	0.447 $\pm$ 0.23
0.2 mM $\text{Ca}^{2+}$	0.477 $\pm$ 0.08	0.122 $\pm$ 0.01	0.355 $\pm$ 0.07
0.5 mM $\text{Ca}^{2+}$	0.386 $\pm$ 0.12	0.073 $\pm$ 0.03	0.313 $\pm$ 0.13
1 mM $\text{Ca}^{2+}$	0.355 $\pm$ 0.09	0.111 $\pm$ 0.10	0.244 $\pm$ 0.12

Data are mean  $\pm$  SD of three separate experiments.

largest part of this difference in inhibitory potency between ChTX and IbTX. Table 4 presents  $\text{ID}_{50}$  data for a series of ChTX mutants in which single amino acids are changed to those found in the corresponding position of IbTX. Most of these single amino acid substitutions produced only small deviations in  $\text{ID}_{50}$  values compared to wild-type ChTX. However, some of the mutants produced pronounced changes in inhibitory properties against the red cell Gardos channel which differed markedly from those reported by Stampe, Kolmakova-Partensky & Miller (1994) against the reconstituted large conductance  $\text{K}_{\text{Ca}}$  (maxi-K) channel from rat skeletal muscle. As shown in Table 4, this is most evident for the mutant W14A, which inhibits the maxi-K channel with 37-fold lower potency than ChTX, but inhibits the human erythrocyte Gardos channel with 3-fold greater potency than ChTX. The ChTX mutant Q18K displayed 5-fold enhanced inhibitory potency against the red cell Gardos channel. In contrast, ChTX mutants T9V and S6D showed decreased inhibitory potency in red cells but increased inhibitory potency against the skeletal muscle channel (Table 4). A double mutant T8S/T9V failed to significantly affect the  $\text{ID}_{50}$  values compared with the wild-type toxin.

ChTX N30Q is altered in a position at which ChTX and IbTX differ, but the Q is not present at this position in IbTX. This mutation produced a large reduction in inhibitory potency ( $\text{ID}_{50} = 1.2 \pm 0.4$  mM in low ionic strength medium and  $79 \pm 39$  mM in physiological saline), but not complete loss of inhibition as observed with IbTX. Studies with  $^{125}\text{I}$ -ChTX binding indicated a moderate reduction in displacement ( $57 \pm 16\%$  of that pro-

duced by ChTX, 10 nM) compared with the lack of displacement observed with IbTX.

$\text{Ca}^{2+}$ -activated  $^{86}\text{Rb}^{+}$  uptake into rabbit erythrocytes, in contrast to human erythrocytes, is partially sensitive to inhibition by IbTX (Brugnara et al., 1993a). We therefore compared the effects of KTX, ChTX, MgTX and ChTX analogues on transport via the Gardos channel in rabbit red cells. As shown in Table 5, there was a close similarity between the inhibitory effects of IbTX and those of the two KTX polypeptides tested. The inhibitory potency of IbTX ( $\text{ID}_{50} = 18 + 7$  nM) was similar to those of KTX (1–37,  $\text{ID}_{50} = 47 + 8$  nM; 1–38,  $\text{ID}_{50} = 38 + 9$  nM). Both KTX and IbTX were considerably less potent inhibitors of  $\text{Ca}^{2+}$ -activated  $^{86}\text{Rb}$  transport in rabbit red cells than ChTX ( $\text{ID}_{50} = 34 \pm 15$   $\mu\text{M}$ ).

ChTX analogues with single amino acid mutations were also studied in the rabbit red cell. Among these were charge-neutralizing mutations in several lysine residues previously studied by measuring inhibition of changes in  $E_m$  induced by A23187 in the presence of  $\text{CaCl}_2$  (Brugnara et al., 1993a). However, their  $\text{ID}_{50}$  values for inhibition of  $\text{Ca}^{2+}$ -activated  $\text{K}^{+}$  flux had not been measured. The K11QE12Q, H21Q, K31Q, S6D, and T9V mutants displayed a 5–20-fold reduction in inhibitory potency, whereas Q18K showed no change in inhibitory potency. These findings are consistent with important roles of the N30 and K31 residues of ChTX in the high affinity interaction of the toxin with both human and rabbit red cells.

## Discussion

This pharmacological characterization of peptide toxin binding to and inhibition of the red cell Gardos channel in human and rabbit has yielded several novel findings. First, KTX and MgTX, which fail to inhibit large conductance  $\text{K}_{\text{Ca}}$  channels, have inhibitory activity against the red cell Gardos channel. In contrast, IbTX, which in excitable tissues is active only against large conductance  $\text{K}_{\text{Ca}}$  channels and not against voltage-gated  $\text{K}^{+}$  channels, is inactive against the human Gardos channel but shows activity against the rabbit Gardos channel (Brugnara et al., 1993a). Second, the effects of single residue mutations in ChTX on inhibition of the erythrocyte Gardos channel differ in magnitude and direction from their effects on the maxi-K channel of skeletal muscle. Third, the marine toxin *Styrodactyla* toxin (StK), originally described as an inhibitor of voltage-gated  $\text{K}^{+}$  channels (Karlsson et al, 1993), is a nanomolar potency inhibitor of the voltage-insensitive,  $\text{Ca}^{2+}$ -gated Gardos channel. Fourth, apamin and scyllatoxin (ScyTX), known to date only as inhibitors of low conductance  $\text{K}^{+}$  channels of neuronal and other cells, displaced at least a portion of  $^{125}\text{I}$ -ChTX with low and moderate potency, respectively, whereas neither exhibited functional blockade of the Gardos channel.



**Table 4.** Inhibition of Ca<sup>2+</sup>-activated <sup>86</sup>Rb<sup>+</sup> transport and of <sup>125</sup>I-ChTX binding in human erythrocytes by ChTX variants mutated in single amino acids

	Human erythrocytes		Mutant/ChTX ratio			<sup>125</sup> I-ChTX Displacement %
	Inhibition %	ID <sub>50</sub> (app) (pM)	ID <sub>50</sub> ratio RBC	RSM	RBC/RSM*	
Wild-type	100%	32 ± 8	1	1	1	72 ± 5
N4D	98.3	73 ± 30	2.25	0.84	2.7	66 ± 21
S6D	98.9	102 ± 37	3.14	0.60	5.2	48 ± 17
T8S	99.8	21 ± 13	0.65	0.35	1.9	55 ± 8
T9V	97.8	86 ± 25	2.97	0.23	12.9	51 ± 28
T8S/T9V	98	21 ± 10	0.72	0.55	1.3	49 ± 25
Q18K	98.3	7 ± 2	0.21	1.3	0.16	72 ± 28
S24D	98	26 ± 29	(0.90)	1.6	0.6	57 ± 20
N30Q	94.2	1200 ± 400	37.5	24	1.5	57 ± 16
W14A	99.3	11 ± 3	0.35	37	0.009	85 ± 21

\* Data for the rat skeletal muscle (RSM) channel are from Stampe et al. (1994), and were measured at physiological ionic strength. Flux inhibition in red cells was measured in low ionic strength conditions. Percentage of <sup>125</sup>I-ChTX displacement was measured with 50 pM <sup>125</sup>I-ChTX in the presence of 10 nM unlabeled competitor toxin. 100% displacement was taken as the displacement by 50 nM unlabeled ChTX.

The human red cell Gardos channel displays a distinct spectrum of peptide toxin specificities and potencies compared to other K<sup>+</sup> channels, including Ca<sup>2+</sup>-gated K<sup>+</sup> channels. This is indicated by the rank order of toxin potency in low ionic strength conditions (ChTX > StK > MgTX > KTX > IbTX = 0), which contrasts with the rank-order sequence (IbTX, ChTX, KTX, NTX, MgTX) proposed from studies of smooth and skeletal muscle to reflect decreasing specificity for Ca<sup>2+</sup>-gated K<sup>+</sup> channels and increasing specificity for voltage-gated K<sup>+</sup> channels (Romi et al., 1993).

Our data suggest that KTX specifically interacts with the human and rabbit red cell Gardos channels. KTX resembles ChTX in its pH-dependence and ionic strength dependence of binding and blockade (Table 1 and 3). However, the inhibitory potency of KTX is lower than that of ChTX (Table 2). Moreover, the impairment of KTX-mediated blockade by elevations of intracellular or of extracellular K<sup>+</sup> is more potent and more complete than the impairment of ChTX-mediated (Fig. 2). Thus, the structural differences between ChTX and KTX are reflected in distinctions in their high affinity interactions with the Gardos channel. Moreover, flux inhibition and binding data both indicate that KTX 1–37 has a slightly higher affinity than does KTX 1–38 for the human red cell Gardos channel. There is a relatively good correspondence between inhibition of <sup>86</sup>Rb<sup>+</sup> influx by KTX and toxin displacement of the radioligands <sup>125</sup>I-ChTX (ID<sub>50</sub> = 1.1 ± 0.3 nM and 4.2 ± 0.4 nM, 1–37 and 1–38 KTX, respectively) and <sup>125</sup>I-KTX (ID<sub>50</sub> = 4.9 ± 1.1 nM and 8.2 ± 4.0 nM, KTX 1–37 and ChTX, respectively). In human red cells, the ID<sub>50</sub> values for ChTX displacement of either <sup>125</sup>I-KTX (8.2 ± 4.0 nM) or <sup>125</sup>I-ChTX (0.3 ± 0.1 nM) differ by more than one order of magnitude, thus replicating the difference in flux inhibitory potencies between ChTX and KTX.

In contrast, in rat brain synaptosomes (Romi et al., 1993) the concentrations for half-maximal displacement of <sup>125</sup>I-KTX by ChTX (8 nM) and KTX (10 pM) differed much more markedly. Together with the displacement of <sup>125</sup>I-KTX by DTX (ID<sub>50</sub> = 8 pM) these data suggest a partial overlap between KTX and DTX binding sites on neuronal voltage-gated K<sup>+</sup> channels, with little overlap between binding sites for KTX and ChTX (Romi et al., 1993) such as observed here in red cells.

Among toxin inhibitors of voltage-gated K<sup>+</sup> channels, MgTX and StK showed significant inhibition of the Gardos channel, whereas DTX displayed no inhibition. Inhibition by MgTX was present in low ionic strength conditions, but absent in normal saline. MgTX has been shown to interact specifically with the lymphocyte K<sub>v</sub>1.3 channel (ID<sub>50</sub> of 30–100 pM for inhibition of K<sup>+</sup> currents and 36 pM for displacement of bound <sup>125</sup>I-ChTX), while MgTX had no effect on intermediate-conductance Ca<sup>2+</sup>-gated K<sup>+</sup> channels of lymphocytes (Garcia et al., 1993). The recently described marine toxin StK also displayed significant inhibition of Ca<sup>2+</sup>-activated K<sup>+</sup> transport in the red cell and specifically displaced bound <sup>125</sup>I-ChTX (Table 2). Previously, StK was reported to block voltage-gated K<sup>+</sup> channels (Karlsson et al., 1993; Kem et al., 1989).

Since ChTX is a potent blocker of the human red cell Gardos channel, whereas the 68% identical IbTX is inactive as an inhibitor, ChTX variants mutated in single residues to the corresponding IbTX residue were tested in an attempt to localize one or several residues which might be most important in determining the difference in inhibitory potency between these two toxins. None of the tested single amino acid changes in ChTX reproduced the complete loss of activity seen for IbTX in human red cells. However, the effects of the tested mutations did reveal differences in the response of the red

**Table 5.** Inhibition of  $\text{Ca}^{2+}$ -activated  $^{86}\text{Rb}^+$  transport into rabbit red cells and  $^{125}\text{I}$ -ChTX binding by different peptide toxins

Toxin	$\text{Ca}^{2+}$ -activated $^{86}\text{Rb}^+$ influx		$^{125}\text{I}$ -ChTX specific binding Displacement by 10 nM toxin (%)
	Inhibition (%)	$\text{ID}_{50}(\text{app})$ nM	
ChTX	100	$0.034 \pm 0.015$	73
StK	94	$1.97 \pm 0.55$	60
MgTX	94	$3.4 \pm 0.6$	63
IbTX	50	$18 \pm 7$	53
KTX, 1–37	43	$47 \pm 8$	n.d.
KTX, 1–38	45	$38 \pm 9$	54
ChTX mutants			
K11QE12Q	99	$0.24 \pm 0.08$	n.d.
H21Q	98	$0.26 \pm 0.16$	n.d.
K31Q	87	$0.52 \pm 0.43$	n.d.
S6D	97	$0.25 \pm 0.03$	43
T9V	88	$0.15 \pm 0.04$	34
Q18K	99	$0.023 \pm 0.02$	63
N30Q	94	$2.0 \pm 0.7$	32
W14A	99	$0.006 \pm 0.003$	64

Flux inhibition in red cells was measured in low ionic strength conditions. Percentage of  $^{125}\text{I}$ -ChTX displacement was measured with 50 pM  $^{125}\text{I}$ -ChTX in the presence of 10 nM unlabeled competitor toxin. 100% displacement was taken as the displacement by 50 nM unlabeled ChTX. Data are the average of three determinations with a C.V. varying between 5 and 10%. n.d., not determined.

cell Gardos channel from those previously reported (Stampe et al., 1994) for the skeletal muscle maxi-K channel in lipid bilayer (Table 4). Three such mutants were of particular note. S6D was 3-fold less potent in the red cell, but nearly 2-fold more potent in skeletal muscle. 9V was also 3-fold less potent in the red cell, but nearly five times more potent in skeletal muscle. However, the double mutation T8S/T9V abolished this difference between red cells and skeletal muscle. Most remarkable was the W14A mutation, which altered a residue in which ChTX and IbTX do not differ. This mutant was 3-fold more potent in the red cell than wild-type ChTX, in contrast to its 37-fold lower potency in skeletal muscle. The alanine substitution favored binding to the red cell channel while destabilizing binding to the skeletal muscle channel. In the voltage-gated  $\text{K}^+$  channel Kv1.3, W14 of ChTX has been modeled adjacent to G380 at the outer edge of the tetrameric channel's external vestibule (K.G. Chandy, *personal communication*). ChTX K31 is situated near G380 in the diagonally opposing Kv1.3 protomer within the tetramer. ChTX T8 is adjacent to a third G380 of the tetramer, similar to its adjacency to the equivalent F425 in Shaker (Goldstein, Pheasant & Miller, 1994). However, the *slowpoke*  $\text{Ca}^{2+}$ -gated  $\text{K}^+$  channel sequences of *Drosophila*, mouse, and human (Pallanck & Ganetzky, 1994) bear minimal homology to Kv1.3 in this ecto-loop between S5 and the pore.

The data presented in this and previous papers have indicated an important role in  $\text{K}^+$  channel blockade for the N30 and K31 residues of ChTX. Glutamine substitution in either position leads to a large reduction in inhibition of transport via the Gardos channel. ChTX, KTX and IbTX exhibit strong sequence conservation among aa 27–37. The importance of the C-terminal regions of these toxins for channel interaction has been confirmed by studies of chimeric toxins (Giangiacoia et al., 1993). K27 has been already shown to be a crucial residue for the interaction with the channel (Park & Miller, 1992). Other crucial residues in the C-terminal domain, as defined by Stampe et al. (1994) are R25, M29, N30, R34 and Y36. ChTX iodination at Y36 leads to significant reduction in inhibitory potency against the Gardos pathway in conditions of low, but not physiologic ionic strength (Brugnara et al., 1993a). Mutations at residue 30, which differs between ChTX and IbTX, and at residue 31 (Brugnara et al., 1993a), which differs between ChTX and KTX, also reduce toxin inhibitory potency for  $^{86}\text{Rb}$  transport and  $^{125}\text{I}$ -ChTX displacement.

Excised patch studies of frog erythrocyte membrane have shown the presence of at least two different types of  $\text{K}^+$  channels, which differ in unitary conductance (18 and 38 pS). However, the smaller of the two showed only slight dependence on internal  $\text{Ca}^{2+}$  and variable stimulation by hypotonicity (Hamill, 1983). Human red cell patches display a single type of  $\text{Ca}^{2+}$ -activated  $\text{K}^+$  current characterized by a zero-current unitary conductance of approximately 20 pS (Grygorczyk et al., 1984; Christopherson, 1991). The presence of three types of  $\text{Ca}^{2+}$ -activated  $\text{K}^+$  channels has been recently reported for human red cells, but only one of these currents has been characterized in detail (Leinders et al., 1992). The relationship between the high-affinity interaction of  $^{125}\text{I}$ -ChTX with red cells and the  $\text{Ca}^{2+}$ -activated  $\text{K}^+$  channel(s) remains unproven. However, the difference in IbTX sensitivity between human and rabbit red cells may provide a means to assess this relationship with greater resolution.

The behavior of ScyTX and apamin may allow an additional means to subtype red cell  $\text{K}_{\text{Ca}}$  channels. ScyTX and apamin have been characterized as inhibitors of low-conductance, apamin-sensitive  $\text{K}_{\text{Ca}}$  channels, especially those of the central nervous system (Castle, Haylett & Jenkinson, 1989; Karlsson et al., 1993). In the brain, the two peptides have similar but nonidentical physiological and anatomic patterns of inhibition. ScyTX and ChTX share a common structural motif consisting of a  $\beta$ -sheet connected to an  $\alpha$ -helix by three disulfide bridges (Martins et al., 1990; Bontems et al., 1991; Pagel & Wemmer 1994). However, the binding of apamin and ScyTX to small conductance  $\text{Ca}^{2+}$ -activated  $\text{K}^+$  channels required the toxins' alpha-helix regions (Wadsworth et al., 1994). This region was not essential for the binding of ChTX and KTX to  $\text{Ca}^{2+}$ -activated  $\text{K}^+$

channels of large and intermediate conductance (Stampe et al., 1994; Romi et al., 1993).

Thus, the lack of inhibitory activity of ScyTX and apamin on the Gardos channel was not surprising. However, the ability of ScyTX and apamin to displace a portion of specifically bound  $^{125}\text{I}$ -ChTX with modest potency was unexpected, and suggests possible structural similarity between apamin-sensitive  $\text{K}_{\text{Ca}}$  channels and at least a fraction of red cell  $^{125}\text{I}$ -ChTX binding sites.

The interactions between specifically bound  $^{125}\text{I}$ -ChTX and ScyTX or apamin may be interpreted as evidence for overlapping but nonidentical binding sites on the Gardos channel. Alternatively, ScyTX binding to a channel-associated protein may prevent  $^{125}\text{I}$ -ChTX binding to the channel without itself inducing blockade. The effect of ScyTX indicates that not all  $^{125}\text{I}$ -ChTX binding sites on the red cell are physiologically equivalent.

Recent data suggest that smooth muscle BK channels have a beta subunit which contributes to  $^{125}\text{I}$ -ChTX binding (Knaus et al., 1994). However, mslo alpha subunit expressed alone in *Xenopus* oocytes displayed potent blockade by IbTX (Butler et al., 1993). The existence of beta subunits for the red cell Gardos channel, their possible contribution to  $^{125}\text{I}$ -ChTX binding sites, and their possible relationship to  $^{125}\text{I}$ -ChTX displacement by ScyTX, remains to be investigated.

In conclusion, the interaction between venom peptide toxins and the red cell Gardos pathway indicates that this channel differs pharmacologically in several interesting ways from other  $\text{Ca}^{2+}$ -gated  $\text{K}^{+}$  channels studied to date.

We thank Dr. Chris Miller of Brandeis University for generously providing recombinant ChTX mutants, Dr. Maria Garcia of Merck Research Laboratories for MgTX and Dr. Regine Romi of Laboratoire d'Ingenierie des Proteines (Marseille, France) for synthetic KTX<sub>1-37</sub> and KTX<sub>1-38</sub>. This research was supported by grant HL-15157 from the National Institutes of Health.

## References

- Alvarez, J., Montero, M., Garcia-Sancho J. 1992. High affinity inhibition of  $\text{Ca}^{2+}$ -dependent  $\text{K}^{+}$  channels by cytochrome P-450 inhibitors. *J. Biol. Chem.* **267**:11789–11793
- Auguste, P., Hugues, M., Graves, B., Gesquires, J.C., Maes, P., Tartar, A., Romey, G., Schweitz, H., Lazdunski, M. 1990. Leiurotoxin I (Scyllatoxin), a peptide ligand for  $\text{Ca}^{2+}$ -activated  $\text{K}^{+}$  channels. *J. Biol. Chem.* **265**:4753–4759
- Bednarek, M.A., Bugianesi, R.M., Leonard, R.J., Felix, J.P. 1994. Chemical synthesis and structure-function studies of margatoxin, a potent inhibitor of voltage-dependent potassium channel in human T lymphocytes. *Biochem. Biophys. Res. Comm.* **198**:619–625
- Bontems, F., Roumestand, C., Boyot, P., Gilquin, B., Doljansky, Y., Menez, A., Toma, F. 1991a. Three dimensional structure of natural charybdotoxin in aqueous solution by 1H-NMR. *Eur. J. Biochem.* **196**:19–28
- Bontems, F., Roumestand, C., Gilquin, B., Menez, A., Toma, F. 1991b. Refined structure of charybdotoxin: common motifs in scorpion toxins and insect defensins. *Science* **254**:1521–1523
- Bookchin, R.M., Ortiz, O.E., Lew, V.L. 1991. Evidence for a direct reticulocyte origin of dense red cells in sickle cell anemia. *J. Clin. Invest.* **87**:113–124
- Brugnara C., Bunn, H.F., Tosteson, D.C. 1986. Regulation of erythrocyte cation and water content in sickle cell anemia. *Science* **232**:388–390
- Brugnara, C., De Franceschi, L., Alper, S.L. 1993a.  $\text{Ca}^{2+}$ -activated  $\text{K}^{+}$  transport of human and rabbit erythrocytes: Comparison of binding and transport inhibition by scorpion toxins. *J. Biol. Chem.* **268**:8760–8768
- Brugnara, C., De Franceschi, L., Alper, S.L. 1993b. Inhibition of  $\text{Ca}^{2+}$ -dependent  $\text{K}^{+}$  transport and cell dehydration in sickle erythrocytes by clotrimazole and other imidazole derivatives. *J. Clin. Invest.* **92**:520–526
- Butler, A., Tsunoda, S., McCobb, D.P., Wei, A., Salkoff, L. 1993. mslo, a complex mouse gene encoding "maxi" calcium-activated potassium channels. *Science* **261**:221–224
- Candia, S., Garcia, M.L., Latorre, R. 1992. Mode of action of iberiotoxin, a potent blocker of the large conductance  $\text{Ca}^{2+}$ -activated  $\text{K}^{+}$  channel. *Biophys. J.* **63**:583–590
- Castle, N.A., Haylett, D.G., Jenkinson, D.H. 1989. Toxins in the characterization of potassium channels. *Trends. Neurosci.* **12**:59–65
- Christopherson, P. 1991. Ca-activated K channel from human erythrocyte membranes: single channel rectification and selectivity. *J. Membrane Biol.* **119**:75–83
- Crest, M., Jacquet, G., Gola, M., Zerrouk, H., Benslimane, A., Rochat, H., Mansuelle, P., Martin-Eclair, M.F. 1992. Kaliotoxin, a novel peptidyl inhibitor of neuronal BK-Type  $\text{Ca}^{2+}$ -activated  $\text{K}^{+}$  channels characterized from *Androctonus mauretanicus mauretanicus* Venum. *J. Biol. Chem.* **267**:1640–1647
- Deutsch, C., Price, M., Lee, S., King, V.F., Garcia, M.L. 1991. Characterization of high affinity binding sites for charybdotoxin in human T lymphocytes. *J. Biol. Chem.* **266**:3668–3674
- Ellory, J.C., Kirk, K., Culliford, S.J., Nash, G.B., Stuart, J. 1992. Nifedipine is a potent inhibitor of the  $\text{Ca}^{2+}$ -activated  $\text{K}^{+}$  channel of human erythrocytes. *FEBS Lett.* **296**:219–221
- Galvez, A., Gimenez-Gallego, G., Reuben, J.P., Roy-Contancin, L., Feigenbaum, P., Kaczorowski, G.J., Garcia, M.L. 1990. Purification and characterization of a unique, potent, peptidyl probe for the high conductance calcium-activated potassium channel from venom of the scorpion *Buthus tamulus*. *J. Biol. Chem.* **265**:11083–11090
- Garcia, M.L., Garcia-Calvo, M., Hidalgo, P., Lee, A., MacKinnon, R. 1994. Purification and characterization of three inhibitors of voltage-dependent  $\text{K}^{+}$  channels from *Leiurus Quinquestratus* var. *Hebraeus* venom. *Biochem.* **3**:6834–6839
- Garcia-Calvo, M., Knaus, H-G., McManus, O.B., Giangiacomo, K.M., Kaczorowski, G.J., Garcia, M.L. 1994. Purification and reconstitution of the high-conductance calcium-activated potassium channel from tracheal smooth muscle. *J. Biol. Chem.* **269**:676–782
- Garcia-Calvo, M., Leonard, R.J., Novick J., Stevens, S.P., Schmalhofer, W., Kaczorowski, J., Garcia, M.L. 1993. Purification, characterization and biosynthesis of margatoxin, a component of *Centruroides margaritatus* venom that selectively inhibits voltage-dependent K channels. *J. Biol. Chem.* **268**:18866–18874
- Gardos, G. 1959. The permeability of human erythrocytes to potassium. *Acta Physiol. Acad. Sci. Hung.* **10**:185–189
- Giangiacomo, K.M., Sugg, E.E., Garcia-Calvo, M., Leonard, R.J., McManus, O.B., Kaczorowski, G.J., Garcia, M.L. 1993. Synthetic charybdotoxin-iberiotoxin chimeric peptides define toxin binding sites on calcium-activated and voltage-dependent potassium channels. *Biochem.* **32**:2363–2370
- Gimenez-Gallego, G., Navia, M.A., Reuben, J.P., Katz, G.M., Kaczorowski, G.J., Garcia, M.L. 1988. Purification, sequence, and model

- structure of charybdotoxin, a potent selective inhibitor of calcium-activated potassium channels. *Proc. Natl. Acad. Sci. USA* **85**:3329–3333
- Goldstein, S.A., Pheasant, D.J., Miller, C. 1994. The charybdotoxin receptor of a Shaker K<sup>+</sup> channel: peptide and channel residues mediating molecular recognition. *Neuron* **12**:1377–1388
- Grissmer, S., Nguyen, A.N., Aiyar, J., Hanson, D.C., Mather, R.J., Gutman, G.A., Karmilowicz, M.J., Auperin, D.D., Chandy, K.G. 1994. Pharmacological characterization of five cloned voltage-gated K<sup>+</sup> channels, types Kv1.1, 1.2, 1.3, 1.5, and 3.1, stably expressed in mammalian cell lines. *Molec. Pharm.* **45**:1227–1234
- Grissmer, S., Nguyen, A.N., Cahalan, M.D. 1993. Calcium-activated potassium channels in resting and activated human T lymphocytes. Expression levels, calcium dependence, ion selectivity, and pharmacology. *J. Gen. Physiol.* **102**:601–630
- Grygorczyk, R., Schwarz, W. 1983. Properties of the Ca<sup>2+</sup>-activated K<sup>+</sup> conductance of human red cells as revealed by the patch-clamp technique. *Cell Calcium* **4**:499–510
- Grygorczyk, R., Schwarz, W., Passow, H. 1984. Ca<sup>2+</sup>-activated K<sup>+</sup> channels in human red cells: Comparison of single-channel currents with ion fluxes. *Biophys. J.* **45**:693–698
- Halperin, J.A., Brugnara, C., Nicholson-Weller, A. 1989a. Ca<sup>++</sup> activated K<sup>+</sup> efflux limits complement mediated lysis of human erythrocytes. *J. Clin. Invest.* **83**:1466–1471
- Halperin, J.A., Brugnara, C., Tosteson, M.T., Van Ha, T., Tosteson, D.C. 1989b. Voltage activated cation transport in human erythrocytes. *Am. J. Physiol.* **257**:C986–C996
- Hamill, O.P. 1983. Potassium and chloride channels in red blood cells. In: Single Channel Recording. B. Sackmann and E. Neher editors. pp. 451–471. Plenum Press, New York
- Heinz, A., Passow, H. 1980. Role of external potassium in the calcium-induced potassium efflux from human red blood cell ghosts. *J. Membrane Biol.* **57**:119–131
- Heinz, A., Hoffman, J.F. 1990. Membrane sidedness and the interaction of H<sup>+</sup> and K<sup>+</sup> on Ca<sup>2+</sup>-activated K<sup>+</sup> transport in human red blood cells. *Proc. Natl. Acad. Sci. USA* **87**:1998–2002
- Johnson, B.A., Sugg, E.E. 1992. Determination of the three-dimensional structure of iberiotoxin in solution by <sup>1</sup>H nuclear magnetic resonance spectroscopy. *Biochem.* **31**:8151–8159
- Kaji, D. 1990. Nifedipine inhibits calcium-activated K transport in human erythrocytes. *Am. J. Physiol.* **259**:C332–C339
- Karlsson, E., Harvey, A.L., Aneiros, A., Castaneda, O. 1993. Potassium channel toxins from marine animals. *Toxicon* **31**:504a
- Kem, W.R., Parten, B., Pennington, M.W., Price, D.A., Dunn, B.M. 1989. Isolation, characterization and amino acid sequence of a polypeptide neurotoxin occurring in the sea anemone *Stichodactyla helianthus*. *Biochem.* **28**:3483–3489
- Knaus H.G., Folander, K., Garcia-Calvo, M., Garcia, M.L., Kaczorowski, G.J., Smith, M., Swanson, R. 1994. Primary sequence and immunological characterization of b-subunit of high conductance Ca<sup>2+</sup>-activated K<sup>+</sup> channel from smooth muscle. *J. Biol. Chem.* **269**:17274–17278
- Latorre, R., Oberhauser, A., Labarca, P., Alvarez, O. 1989. Varieties of calcium-activated potassium channels. *Annu. Rev. Physiol.* **51**:385–399
- Leinders, T., van Kleef R.G.D.M., Vijverberg, H.P.M. 1992. Single Ca<sup>2+</sup>-activated K<sup>+</sup> channels in human erythrocytes: Ca<sup>2+</sup>-dependence of opening frequency but not of open lifetimes. *Biochim. Biophys. Acta* **1112**:67–74
- Lew, V.L., Freeman, C.J., Ortiz, O.E., Bookchin, R.M. 1991. A mathematical model of the volume, pH and ion content regulation in reticulocytes. *J. Clin. Invest.* **87**:100–112
- Martins, J.C., Zhang, W.G., Tartar, A., Lazdunski, M., Borremans, F.A. 1990. Solution conformation of leurotoxin I (Scyllatoxin) by 1H nuclear magnetic resonance. resonance assignment and secondary structure. *FEBS Lett.* **260**:249–253
- Miller, C., Mockzydowski, R., Latorre, R., Phillips, M. 1985. Charybdotoxin, a protein inhibitor of single Ca<sup>2+</sup>-activated K<sup>+</sup> channels from mammalian skeletal muscle. *Nature* **313**:316–318
- Pagel, M.D., Wemmer, D.E. 1994. Solution structure of a core peptide derived from scyllatoxin. *PROT. Struct. Funct. Gen.* **18**:205–215
- Pallanck, L., Ganetzky, B. 1994. Cloning and characterization of human and mouse homologs of the *Drosophila* calcium-activated potassium channel gene, slowpoke. *Human Mol. Gen.* **3**:1239–1243
- Park, C.S., Haudoorff, S.F., Miller C. 1991. Design, synthetic and functional expression of a gene for charybdotoxin, a peptide blocker of K<sup>+</sup> channels. *Proc. Natl. Acad. Sci. USA* **88**:2046–2050
- Park, C.S., Miller, C. 1992. Interaction of charybdotoxin with permeant ions inside the pore of a K<sup>+</sup> channel. *Neuron* **9**:307–313
- Reichstein, E., Rothstein, A. 1981. Effects of quinine on Ca<sup>++</sup>-induced K<sup>+</sup> efflux from human red blood cells. *J. Membrane Biol.* **59**:57–63
- Romi, R., Crest, M., Gola, M., Sampieri, F., Jacquett, G., Zerrouk, H., Mansuelle, P., Sorokine, O., Van Dorsselaer, A., Rochat, H., Martin-Euclaire, M.F., Van Rietschoten, J. 1993. Synthesis and characterization of kaliotoxin. Is the 26–32 sequence essential for potassium channel recognition? *J. Biol. Chem.* **268**:26302–26309
- Simons, T.J. 1976. Carbocyanine dyes inhibit Ca-dependent K efflux from human red cell ghosts. *Nature* **264**:467–469
- Stampe, P., Kolmakova-Partensky, L., Miller, C. 1994. Intimation of K<sup>+</sup> channel structure from a complete functional map of the molecular surface of charybdotoxin. *Biochem.* **33**:443–450
- Stampe, P., Vestergaard-Bogind, B. 1985. The Ca<sup>2+</sup>-sensitive K<sup>+</sup>-conductance of the human red cell membrane is strongly dependent on cellular pH. *Biochem. Biophys. Acta* **815**:313–321
- Tauc, M., Congar, P., Poncet, V., Merot, J., Vita, C., Poujeol, P. 1993. Toxin pharmacology of the large-conductance Ca<sup>2+</sup>-activated K<sup>+</sup> channel in the apical membrane of rabbit proximal convoluted tubule in primary culture. *Pfluegers Arch.* **425**:126–133
- Vasquez, J., Feigenbaum, P., Katz, V.F., Reuben, J.P., Roy-Contacin, L., Slaughter, R.S., Kaczorowski, G.J., Garcia, M.L. 1989. Characterization of high affinity binding sites for charybdotoxin in sarcolemmal membranes from bovine aortic smooth muscle. *J. Biol. Chem.* **264**:20902–20909
- Wadsworth, J.D., Doorty, K.B., Strong, P.N. 1994. Comparable 30-kDa apamin binding polypeptides may fulfill equivalent roles with putative subtypes of small conductance Ca<sup>2+</sup>-activated K<sup>+</sup> channels. *J. Biol. Chem.* **269**:18053–18061
- Wolff, D., Cecchi, X., Spalvins, A., Canessa, M. 1988. Charybdotoxin blocks with high affinity the Ca-activated K<sup>+</sup> channel of Hb A and Hb S red cells: individual differences in the number of channels. *J. Membrane Biol.* **106**:243–252